

# 1 Glider data collected during the Algerian Basin Circulation 2 Unmanned Survey

3  
4 Yuri Cotroneo<sup>a,\*</sup>, Giuseppe Aulicino<sup>a,b</sup>, Simon Ruiz<sup>c</sup>, Antonio Sánchez Román<sup>c</sup>, Marc Torner Tomàs<sup>d</sup>,  
5 Ananda Pascual<sup>c</sup>, Giannetta Fusco<sup>a,e</sup>, Emma Heslop<sup>f</sup>, Joaquin Tintoré<sup>c,d</sup> and Giorgio Budillon<sup>a,e</sup>  
6  
7

8 *a* Università degli Studi di Napoli “Parthenope”, Centro Direzionale di Napoli, Isola C4, 80143,  
9 Napoli, Italy

10 *b* Università Politecnica delle Marche, Via Brecce Bianche, 12, 60131, Ancona, Italy

11 *c* Instituto Mediterráneo de Estudios Avanzados, IMEDEA(CSIC-UIB),  
12 Carrer de Miquel Marquès, 21, 07190 Esporles, Illes Balears, Spain

13 *d* Balearic Islands Coastal Observing and Forecasting System (SOCIB), Edificio Naorte.  
14 Bloque A, 2º piso, puerta 3, Parc Bit, 07122 Palma, Spain

15 *e* Consorzio Interuniversitario Nazionale per la Fisica delle Atmosfere e delle Idrosfere, CINFAI,  
16 Piazza Nicolò Mauruzi, 17, 62029 Tolentino (MC), Italy

17 *f* Intergovernmental Oceanographic Commission of UNESCO, 7, place de Fontenoy  
18 75732 Paris cedex 07, France  
19  
20

21 \* Corresponding author: Yuri Cotroneo – yuri.cotroneo@uniparthenope.it  
22  
23

## 24 **Abstract**

25  
26 We present data collected in the framework of the Algerian Basin Circulation Unmanned Survey -  
27 ABACUS project. ABACUS main objective is the monitoring of the basin circulation and of the  
28 surface and intermediate water masses physical and biological properties in a key region of the  
29 Mediterranean Sea circulation. Data presented here have been collected through deep glider  
30 cruises in the Western Mediterranean Sea during the autumns of 2014, 2015 and 2016; activities  
31 at sea are expected to be repeated during the coming years, so that the dataset will be extended.  
32 Glider missions were realized in the Algerian Basin, between the Island of Mallorca and the  
33 Algerian Coast. Across the three glider missions, eight repeated transects were obtained which  
34 enabled us to investigate the basin scale circulation and the presence of mesoscale structures  
35 utilising both the adaptive sampling capabilities of the gliders and the higher resolution of the  
36 data.

37 After collection, all data passed a quality control procedure and were then made available through  
38 an unrestricted repository host by the SOCIB Data Centre at <https://doi.org/10.25704/b200-3vf5>.  
39 The actual dataset spans three fall seasons, providing an important contribution to the data  
40 collection in the chronically undersampled Algerian Basin.

41 Temperature and salinity data collected in the first 975 m of the water column allowed us to  
42 identify the main water masses and describe their characteristics improving the understanding of  
43 the dynamics of the region. On the time scale of the project, data show a large variability at the  
44 surface layer and reduced variability at the intermediate and deep layers.

45 Our measurements have been successfully compared to data previously collected in the area from  
46 1909 to 2011. Results showed similar overall distribution, ranges and variability as the historical  
47 data, with no outliers in the surface or deep layers.

48  
49  
50  
51  
52  
53  
54  
55  
56  
57  
58  
59  
60  
61  
62  
63  
64  
65  
66  
67  
68  
69  
70  
71  
72  
73  
74  
75  
76  
77  
78  
79  
80  
81  
82  
83  
84  
85  
86  
87  
88  
89  
90  
91  
92  
93  
94  
95

## 1 Introduction

The southwestern Mediterranean Sea is an important transit region characterized by the presence of both fresh surface waters coming from the Atlantic (Atlantic Water, hereafter AW) and more saline waters which typically reside in the Mediterranean region. At intermediate levels (400 – 1000 m) there is the Levantine Intermediate Water (LIW), typified by subsurface temperature and salinity maxima, while deeper layers (>1000 m) are occupied by the Western Mediterranean Deep Water (WMDW) (Millot, 1999; Millot et al., 2006). Most of the Western Mediterranean is occupied by the Algerian Basin (AB), a wide and deep basin comprised between the Balearic Islands, the Algerian Coast and the Sardinia Channel, where an intense inflow/outflow regime exists and complex circulation patterns take place (e.g., Pascual et al., 2013; Cotroneo et al., 2016; Aulicino et al., 2018). Typically, AW entering through the Strait of Gibraltar flows eastward at the AB surface, mainly inside the Algerian Current (AC), while more saline water masses, formed in the eastern and northern parts of the Mediterranean, flows westward at the intermediate and deep layers (Millot, 1985; Testor et al., 2005). As previously demonstrated by several studies, AW and Mediterranean waters interact at different scales, from basin-scale to mesoscale and sub-mesoscale (Robinson and Golnaraghi, 1994; Fusco et al., 2003; Vidal-Vijande et al., 2011), allowing a high seasonal and interannual variability in the basin. This aspect is favoured by the presence of the AC. After leaving the Alboran Sea (Tintoré et al., 1991), this 30-50 km wide along-slope current flows eastward along the Algerian coast, carrying the AW eastwards (Testor et al., 2005). Typically, the AC becomes unstable along its path due to complex hydrodynamic processes, and forms several meanders which frequently evolves to isolated cyclonic and anticyclonic mesoscale eddies (e.g., Millot, 1985; Moran et al., 2001; Ruiz et al., 2002; Font et al., 2004; Escudier et al., 2016; Cotroneo et al., 2016; Pessini et al., 2018) promoting an intense mesoscale activity all over the AB. These structures present high levels of kinetic energy (Pascual et al., 2013; Escudier, 2016) and impact the distribution of physical and chemical properties of water masses, especially at surface and intermediate depths (Taupier-Letage et al., 2003; Olita et al., 2011).

In the last two decades, both satellites and numerical simulations data have been largely used to study mesoscale processes, partially balancing the scarcity of in situ observations. This improved our knowledge of the large-scale surface features (Vignudelli et al., 2003; Isern-Fontanet et al., 2016), but a complete understanding of mesoscale and submesoscale processes in the basin is still needed. To this aim, frequent dedicated observations at higher horizontal and vertical resolution, along the water column, are essential (Pascual et al., 2017). Multi-platform monitoring strategies, which enable the integration of data from satellites, Autonomous Underwater Vehicles (AUV) and numerical models, have already demonstrated their capabilities in the assessment of oceanographic processes in different regions of the global ocean, such as the Atlantic Ocean (Shcherbina et al., 2015) and the Mediterranean Sea (Carret et al., 2018; Troupin et al., 2018; Pascual et al., 2017; Aulicino et al., 2016). The value of these is improved when implemented along repeated monitoring lines coincident with the satellite groundtracks (Aulicino et al., 2018). Among other AUVs, measurements at small sampling intervals collected through gliders (<5 km spatial resolution) have contributed to several ocean studies (Rudnick, 2016; Heslop et al., 2012), from dynamics (e.g., Ruiz et al., 2009; Bosse et al., 2016; Cotroneo et al., 2016; Thomsen et al., 2016) to physical and biogeochemical exchanges (e.g., Ruiz et al., 2012; Bouffard et al., 2010; Cotroneo et al., 2016; Olita et al., 2017) or assessment of altimetry data (Heslop et al., 2017). However, gliders generally have a limited speed ranging between 0.35 m/s and 0.50 m/s in the horizontal (Griffiths et al., 2002; Rudnick et al., 2004; Jones et al., 2005; Merckelbach et al., 2010) that can arise synopticity problems when monitoring mesoscale phenomena (Rudnick and Cole, 2011; Alvarez

96 and Moure, 2012; Aulicino et al., 2016; Cotroneo et al., 2016) or wide areas (Liblik et al., 2016).  
97 Thus, their combination with reliable satellite products, numerical simulations and, when  
98 available, other platforms such as drifters, ARGO floats and ship-borne CTDs or a multiple glider  
99 missions represent the good strategy for implementing observatories for marine science research  
100 which aim to study basin scale and/or coastal processes (Aulicino et al., 2018) where issues of  
101 synchronicity are a concern.  
102 Furthermore, this integrated glider-based approach is also important for validating new satellite  
103 products, such as the now fully-operational Sentinel-3 mission (Drinkwater and Rebhan, 2007;  
104 Heslop et al., 2017) and the upcoming Surface Water and Ocean Topography (SWOT) wide-swath  
105 radar interferometer (Fu and Ferrari, 2008), where multi-platform data are expected to help  
106 distinguishing noise from small dynamical structures, as a result of cross calibrations between the  
107 different sensors (Bouffard et al., 2010; Pascual et al., 2013).  
108 In this study, we present data collected through three SLOCUM G2 (Figure 1) glider missions  
109 carried out in the AB during fall 2014, 2015 and 2016. These cruises were developed along a  
110 repeated monitoring line set across the AB and allowed the collection of a huge dataset of physical  
111 and biological ocean parameters in the first 975 m of the water column. For each mission, glider  
112 main track was chosen to lie under overflying altimeter satellites tracks, in order to optimize the  
113 inter-comparison of the data from the two platforms. Additionally, during the 2014 and 2015  
114 glider cruises, the sampling track was changed in order to sample specific mesoscale circulation  
115 structures in the area. Even though this study is restricted to a particular area, i.e. the AB, we  
116 strongly believe that the scientific community could use these data to enlarge the knowledge of  
117 the western Mediterranean Sea and to refine the implementation of glider missions and  
118 integrated multi-platform observatories in other regions. Glider characteristics, sensors details,  
119 paths and mission strategies are described in Section 2; data format and quality control  
120 procedures are presented in Section 3. In section 4, a comparison between ABACUS observations  
121 and historical data, as well as sample ABACUS transects, are presented. Finally, Section 5 reports  
122 main conclusions.

123



124

125 *Figure 1. The SLOCUM G2 glider during the ABACUS pre-mission test at sea. Credit M. Torner.*

126

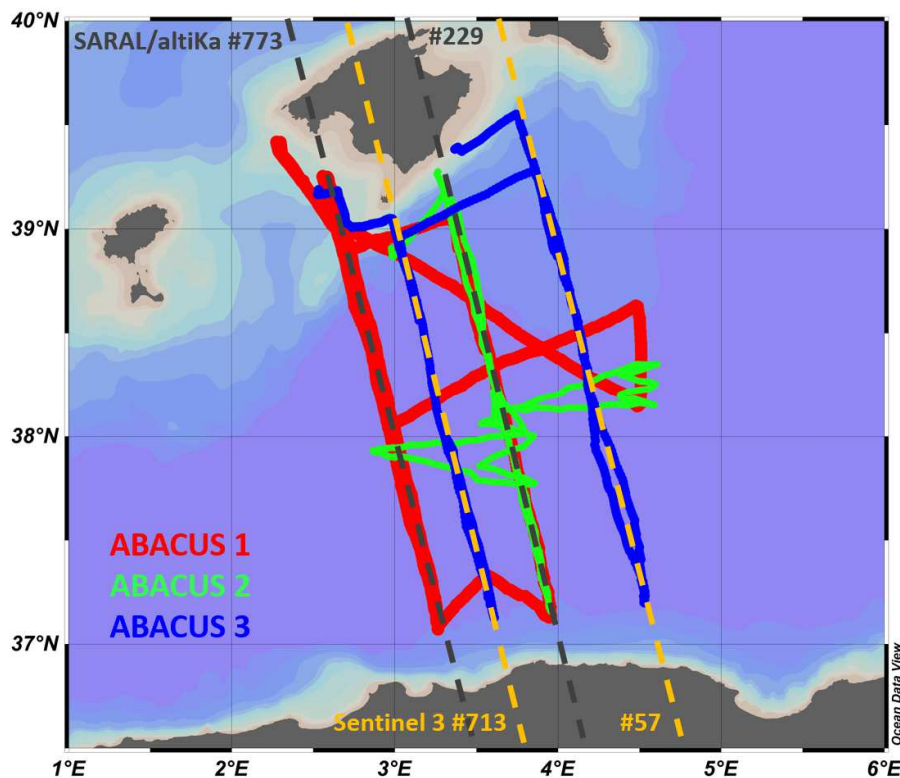
127 **2 Glider field activities and technical details**

128 Gliders are AUV able to provide high resolution hydrographic and bio-chemical measurements.  
129 These vehicles control their buoyancy to allow vertical motion in the water column and make use  
130 of their hydrodynamic shape and small fins to make horizontal motions. Changing the position of  
131 the center of gravity with respect to the center of buoyancy helps controlling both pitch and roll  
132 (Webb et al., 2001). This results in a typical saw-toothed navigation pathway to a maximum depth  
133 of 975 m.

134 During the autumns from 2014 to 2016, three deep SLOCUM G2 glider missions were carried out  
135 in the AB (Figure 2) using two gliders from the same constructor, with the same characteristics and  
136 overpassing the same calibration procedures.

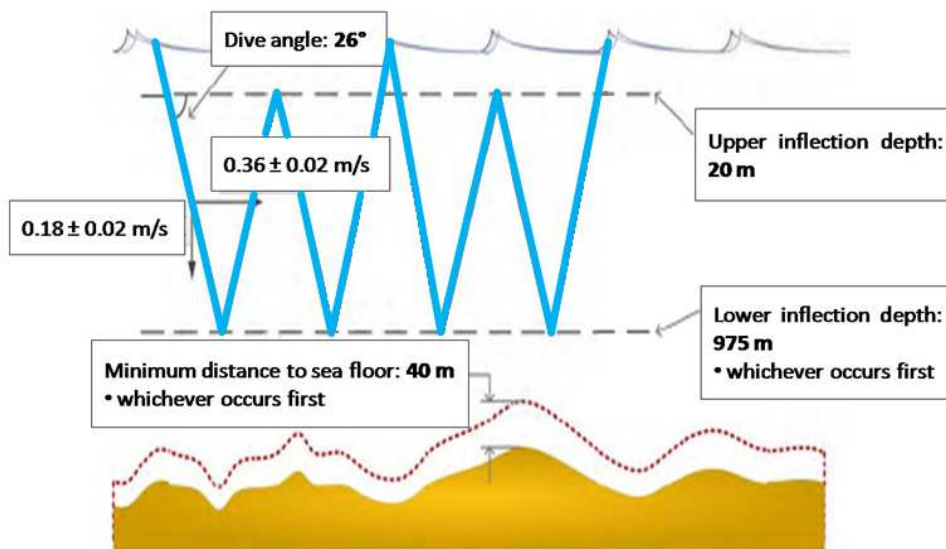
137 ABACUS glider missions were performed in the framework of the SOCIB (Balearic Islands Coastal  
138 Observing and Forecasting System) Glider Facility Open Access Programme and supported by the  
139 Joint European Research Infrastructure network for Coastal Observatories (JERICO) Trans National  
140 Access (TNA). Funding agreements were developed under the JERICO TNA third call (grant No  
141 262584) for ABACUS 1, the SOCIB external access for ABACUS 2 and JERICO-NEXT TNA first call  
142 (grant No. 654410) for ABACUS 3.

143 Up to 2016, a total of 8 repeated transects were realized between the Island of Mallorca and the  
144 Algerian Coast. In 2014 and 2015, after the realization of the defined transects, the glider track  
145 was changed in order to sample specific mesoscale structures in the study area (Figure 2).  
146



147  
148 *Figure 2. Glider tracks during the missions: ABACUS 1 (red dots), ABACUS 2 (green dots) and*  
149 *ABACUS 3 (blue dots). The deviations from the monitoring line were undertaken to sample some*  
150 *mesoscale structures identified through near real time satellite altimetry and SST maps. The*  
151 *groundtracks of the SARAL/AltiKa (grey dashed lines) and Sentinel 3 (yellow dashed lines) satellites*  
152 *over the study area are also showed.*

153 During these cruises ABACUS gliders collected temperature, salinity, turbidity, oxygen and  
154 chlorophyll (CHLA) concentration data in the first 975 m of the water column. Each mission had an  
155 average duration of about 40 days and was always performed between September and December.  
156 In situ data collection was supported by remotely sensed data from different platforms over the  
157 Western Mediterranean Sea. In particular, gridded altimetry data provided by the Archiving,  
158 Validation and Interpretation of Satellite Oceanographic data (AVISO), Sea Surface Temperature  
159 (SST) and CHLA concentration information from MODerate resolution Imaging Spectroradiometer  
160 (MODIS) data acquired by NASA were used to provide a large scale description of the dynamics  
161 and surface water masses. ABACUS field activities were performed in collaboration with SOCIB and  
162 the Mediterranean Institute for Advanced Studies (IMEDEA) using a SLOCUM G2 glider for deep  
163 water (975 m maximum sampling depth) with a vertical speed of  $0.18 \pm 0.02$  m/s, resulting in a  
164 horizontal velocity of about 0.36 m/s. During all missions, the general data acquisition design was  
165 set to dive with a descending angle of  $26^\circ$  between 20 m and maximum depth (Figure 3) with  
166 limited presence and sampling in the layer 0 – 20 m depth. In particular, during the 2014 mission,  
167 data collection in the surface (0-20 m depth) was limited at every third ascending profile, resulting  
168 in a sampling spatial resolution of 8.4 km for depths shallower than 20 m. In 2015 we collected a  
169 complete cast from surface to bottom at about 5 km resolution, as a result of the increased  
170 general resolution of the glider sampling, that was now performed during both upcast and  
171 downcast. Finally, in 2016 we tested glider possibility to sample the entire water column from 0 to  
172 975 m depth at the resolution of 2.8 km. This was obtained sampling during both upcast and  
173 downcast and programming the glider to reach the surface after every cast. The experiment was  
174 successful, but limited in time due to battery constraints. For this reason, during ABACUS 3, the  
175 layer between 0 and 20 m depth is sampled at a variable resolution between 2.8 and 8 km.  
176



177  
178 *Figure 3. Glider navigation scheme during the ABACUS missions. The upper inflection depth was*  
179 *changed after the ABACUS 1 mission in order to allow the glider reaching the surface more*  
180 *frequently.*

181

182 As described, the glider was programmed to reach the surface at different rates/spatial resolution  
 183 during the three ABACUS missions and this resulted in a variable resolution of sampling of the very  
 184 surface layer (0 – 20 m depth).

185 Several physical and optical biochemical sensors were carried aboard the glider for measuring the  
 186 ocean temperature, salinity, oxygen, turbidity and CHLA concentration, at different rates  
 187 according to depth. In particular, ABACUS gliders were equipped with a glider-customized CTD by  
 188 Seabird-Scientific (<http://www.seabird.com/glider-payload-ctd>) measuring temperature, salinity  
 189 (derived from conductivity) and depth, and a two-channel combo Fluorometer-Turbidity sensor by  
 190 Wetlabs-Instruments (<http://www.seabird.com/eco-puck>), both of them embedded inside the  
 191 central hull segment of the glider commonly known as the “science-bay”. Additionally, an oxygen  
 192 optode to measure absolute oxygen concentration and saturation (%) by AADI  
 193 (<https://www.aanderaa.com/productsdetail.php?Oxygen-Optodes-2>) was externally mounted on  
 194 the aft, and wet, section of the glider.

195 The accuracy of the measurements, their vertical resolution and depth range vary according to the  
 196 specific instrument and measured variable as reported in Table 1.

197 Temperature, salinity and oxygen data were sampled to full diving depth (0-975 m depth) while  
 198 the acquisition of the other optical parameters ceased at 300 m depth.

199

Parameter	Instrument	Sampling rate (Hz)	Vertical resolution (m)	Depth range (m)	Accuracy	Resolution
Temperature (T), Conductivity (C), Depth (D)	Seabird GPCTD Glider payload pumped CTD	1/2	0.4	-5 to -975	T ± 0.002 °C C ± 0.0003 S/m D ± 0.1% fsr*	T 0.001 °C C 0.00001 S/m D 0.002% fsr*
Oxygen	AADI Optode 5013	1/4	0.8	-5 to -975	<8 µM or 5%	<1 µM
Fluorescence (F), Turbidity (Tu)	WetlabsFLNTUsIk	1/8	1.6	-5 to -150	<b>Sensitivity</b> F 0.015 ÷ 0.123 µg/L Tu 0.005 ÷ 0.123 NTU	
		1/16	3.2	-150 to -300		

200 *Table 1. Sampling rate and vertical resolution of ABACUS gliders data (adapted from Cotroneo et*  
 201 *al., 2016; Aulicino et al., 2018). \* Full Scale Range*

202

203 A specific sampling rate was defined for each instrument (Table 1). Physical parameters  
 204 (temperature and salinity) were sampled at 1/2 Hz, resulting in a vertical resolution of 0.4 m along  
 205 the water column. Oxygen concentration was acquired at 1/4 Hz (vertical resolution 0.8 m) whilst  
 206 turbidity and chlorophyll were sampled at 1/8 Hz until 150 m depth and at 1/16 Hz from that level  
 207 until 300 m depth, with a vertical resolution of 1.6 m and 3.2 m respectively.

208 Calibration processes and regular maintenance were carried out before and after every glider  
 209 mission and guarantee the quality of the measurements. While temperature and salinity sensors  
 210 were regularly calibrated, unfortunately the optical sensors used during the ABACUS missions  
 211 were not calibrated before the cruises. This results into the impossibility to use the derivated-  
 212 variable values as absolute values. Nonetheless, gradients along space, depth and time can  
 213 successfully be observed and discussed.

214 Generally, real time data transmission from the glider can be adaptively configured before and  
 215 during the mission. For the ABACUS missions, it was set to occur at about every 6 hours, in  
 216 correspondence with every second upcast for most of the glider transects. Real time data (having

217 a file size ranging between 20 and 90 Kb) were transmitted using Iridium satellite link and  
218 contained a subset of all measurements, populated taking one out of every three samples for each  
219 parameter. This strategy permitted the retrieval of a first overview of the data collected, as well as  
220 the eventual transmission of new sampling and navigation directives to the glider. The full  
221 resolution dataset remained stored locally inside the glider until the vehicle was physically brought  
222 back to SOCIB facilities once the mission was completed. Then, data were transferred to SOCIB  
223 Data Center where pre-processing, processing and validation were carried out and NetCDF files  
224 created.

225 The structure and content of the ABACUS NetCDF file is described in section 3.

226 The pre-mission activities were carried out at the SOCIB glider facility (Tintoré et al., 2013) and  
227 included all ballasting, pressure tests, compass validation, and adjustment operations needed to  
228 assure the glider capability to reach the surface. This capability is provided by adjusting the overall  
229 weight of the vehicle and by distributing part of that weight so that inclination and roll are neutral  
230 when the glider sets its mechanical actuators (pump, mass shifter, air bladder and fin) in neutral  
231 mode (0 cc, 0 inch, no inflation and 0 rad respectively). That tuning is driven by the hydrographical  
232 characteristics of the target waters to be navigated, i.e. their minimum density, since they  
233 condition the execution of the mentioned operations. Within this scope, the climatological  
234 maximum value of temperature and minimum value of salinity for the studied area and period  
235 have been analysed. These data were used as extreme hydrographic characteristics of the target  
236 waters and allowed us to derive the minimum density ( $1024.0683 \text{ kg/m}^3$ ) needed to precisely tune  
237 the glider for the target waters. This tune up is required in order to make sure that the vehicle will  
238 always be able to break into the surface and to raise its tail above the water to have clear and  
239 robust communications.

240 As regards compass, Merckelbach et al (2008) developed a method to assess the glider compass  
241 error in SLOCUM gliders. This approach has been followed for gliders used during the later  
242 ABACUS experiments. The methodology should take place at any location away from sources of  
243 hard or soft electromagnetic material (e.g. sport ground), thus it was performed in a forest  
244 cleaning to minimize electromagnetic interference effects. Using a wooden platform, the glider  
245 was placed horizontally and a plastic-made compass stand aligned with the true North was used  
246 allowing precise and repetitive heading gradients of 15 degrees. The measurement error was then  
247 estimated by calculating the difference between the heading measured by the glider and the  
248 heading that was physically imposed using the stand. A maximum error of less than 10 degrees  
249 was observed during the three tests so that compass re-calibration was not considered necessary.  
250 All these operations were performed on the two SLOCUM glider used during the ABACUS missions  
251 (SLDEEP001 for 2014 and 2016; SLDEEP000 for 2015) as part of the pre-missions tests and  
252 contributed in assessing the quality of the collected data.

253 The glider tracks were designed to cross the basin from the island of Mallorca (Spain) to about 20  
254 miles off the Algerian coast (Figure 2). The timing of the missions was accurately planned in order  
255 to provide synoptic in situ data with respect to the satellite SARAL/ALtiKa and Sentinel-3A  
256 passages, being also comparable among the different ABACUS missions (Aulicino et al., 2018).

257 In 2014, during the ABACUS 1 mission, three glider transects were completed along the  
258 neighbouring SARAL/ALtiKa groundtracks 229 and 773 from 15<sup>th</sup> September to 19<sup>th</sup> December  
259 2014. The satellite overpassed the glider on 17 September and 26 November 2014 (track 773) and  
260 on 12 December 2014 (satellite track 229). During ABACUS 2 mission, carried on from 18<sup>th</sup>  
261 November to 11<sup>th</sup> December 2015, the glider was overflowed by the SARAL/ALtiKa satellite on 23

262 October, along the groundtrack 229 with the glider halfway along the transect. In fact, analysis of  
263 the data collected during the 2014 mission, highlighted the need of a higher degree of synopticity  
264 between the glider and satellite data. A specific deployment plan was then designed for the  
265 following ABACUS missions in order to have the glider approximately in the middle of the transect  
266 during the satellite passages. The improvement obtained in synopticity are extensively discussed  
267 in (Cotroneo et al., 2016; Aulicino et al., 2018).

268 During October 2014, a deviation from the planned sampling track was realized in order to  
269 investigate the presence and sample a mesoscale eddy (see red butterfly shape track in Figure 2).  
270 The eddy presence was first identified on the basis of near real time satellite altimetry and SST,  
271 then the glider track was modified during one of the glider surface communication periods. The  
272 adaptive sampling capabilities of the glider were then successfully used to perform two full depth  
273 transects across the mesoscale eddy (Cotroneo et al., 2016). After that, the scheduled ABACUS  
274 sampling track was restarted. The same strategy was applied in 2015 when the glider deviated  
275 twice from the planned track to monitor the edge of a possible mesoscale eddy (saw-tooth green  
276 track in figure 2).

277 Finally, during the ABACUS 3 mission was realized from 4<sup>th</sup> November to 23<sup>rd</sup> December 2016 and  
278 two new glider transects were performed along the Sentinel-3A groundtracks 57 and 713. The  
279 latter being located between the SARAL/AltiKa groundtracks 229 and 773 (see Figure 2). During  
280 this mission the glider was overflowed on 12 November 2016 (track 57) and 5 December 2016  
281 (track 713). All the details about dates of the missions and main water masses identified are  
282 reported in Table 2.

283 Resolution of sampling was defined according to the energetic constraints of the platform and to  
284 the scientific aims of the missions, which required high resolution in both horizontal and vertical  
285 directions to monitor large scale, as well as, mesoscale processes. During the ABACUS 1 mission,  
286 the glider was programmed to sample only during downcasts with a final along-track resolution of  
287 almost 4 km once the oblique profiles are projected into the vertical. As a result of the first data  
288 analysis, the sampling plan for the following missions was modified. During ABACUS 2 (2015) and  
289 ABACUS 3 (2016) cruises, both downcasts and upcasts data were collected, thus obtaining an  
290 improved spatial along-track resolution of about 2 km, while diving angle and speed remained  
291 unchanged. Apart from increasing horizontal sampling resolution, this new strategy also has an  
292 effect on data quality, enabling the application of the thermal lag correction developed by Garau  
293 et al. (2011) which requires consecutive up and down profiles of temperature and salinity.

294

### 295 **3 Data quality control**

296 After each mission, data were transferred from the internal glider memory to the SOCIB Data  
297 Center, where data processing was carried out and production of delayed time NetCDF files at  
298 different elaboration levels (i.e., level 0, level 1, level 2) occurred (Troupin et al., 2016; Cusi et al.,  
299 2013) before web dissemination of the data.

300 Each NetCDF file comprises the main cruise information, data and a short abstract. Level 0  
301 contains the raw data collected by the glider without any elaboration or correction and organized  
302 in vectors. Level 1 includes data regularized, corrected and/or derived from raw glider data. Each  
303 variable is stored as sequences of measurements along the glider trajectory, with interpolated  
304 position coordinates to match the times of measurement by the sensor, and with unit conversions  
305 and filters applied. Each variable is described and commented individually. Level 2 dataset includes



306 the regularly sampled vertical profiles generated from depth binning of already processed (level 1)  
307 glider data. The profiles are obtained by interpolation of level 1 data to produce regular  
308 homogeneous and instantaneous profiles from each up or downcast, using the mean time and  
309 position of the corresponding cast for the profile location and time. In this level, each variable is  
310 stored in matrix. Depth increases with the number of rows, with each row corresponding to 1 m  
311 depth, while time and consequently the number of profiles changes along the columns.

312 Delayed mode data processing for level 1 and 2 included thermal lag correction, filtering and 1 m  
313 bin vertical averaging (Troupin et al., 2016). In particular, in level 1 and 2, filters are mainly focused  
314 on the processing of pressure data through a low pass filter and on the interpolation of missing  
315 values. Nevertheless, some unexpected high oxygen concentration and high salinity values, as well  
316 as abrupt temperature value changes, were still present in the surface layer after this standard  
317 quality control protocol. The presence of these doubtful values at the shallower turning depth of  
318 the glider supports the hypothesis of a possible effect of glider navigation phase change on the  
319 sampling capability.

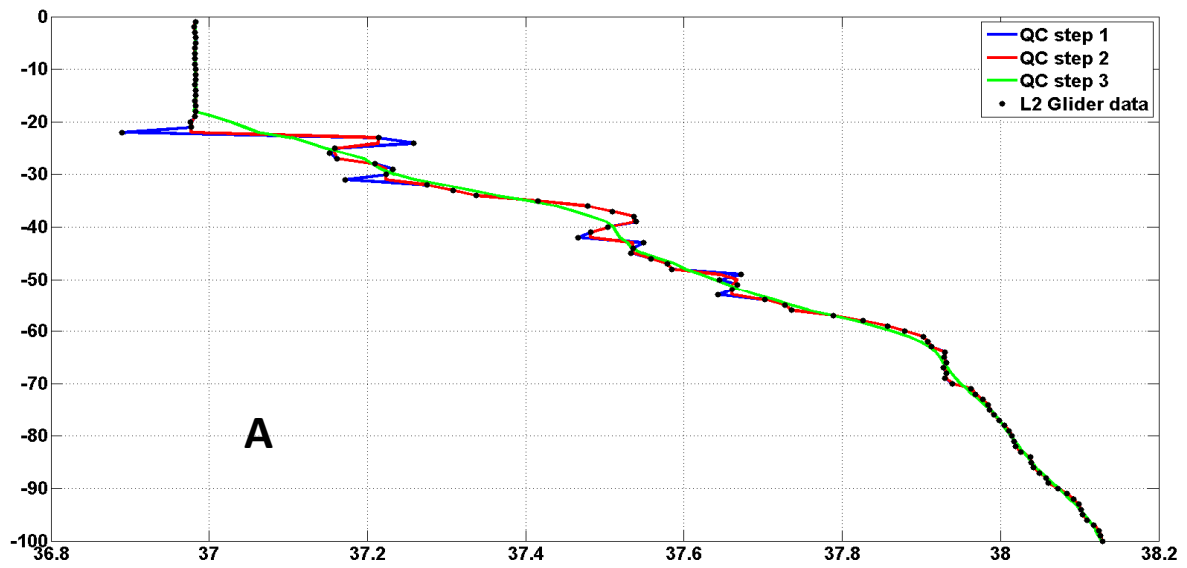
320 For this reason, during the 2015 and 2016 missions, the glider was programmed to reach the  
321 surface after every profile in order to avoid this issue, improve the data collection in the very  
322 surface layer (depth < 20 m) and provide a more suitable dataset for the comparison with satellite  
323 data.

324 Nevertheless, an additional quality control procedure was developed and regularly performed at  
325 University of Naples “Parthenope” on all ABACUS data. In particular, this procedure includes an  
326 additional single-point spike control, the interpolation of single missing data along the profiles, the  
327 application of a dedicated median filter, a 5-point running mean along the depth and, finally, an  
328 iterative comparison between adjacent profiles. This tool allowed us to identify and discard bad  
329 data and artefacts that were still present after the standard quality control. This final product is  
330 indicated as level 3 of the ABACUS dataset. An example of the level 3 elaboration steps is given in  
331 Figure 4. This additional procedure was routinely adopted for the quality control of all ABACUS  
332 glider missions for each geophysical parameter.

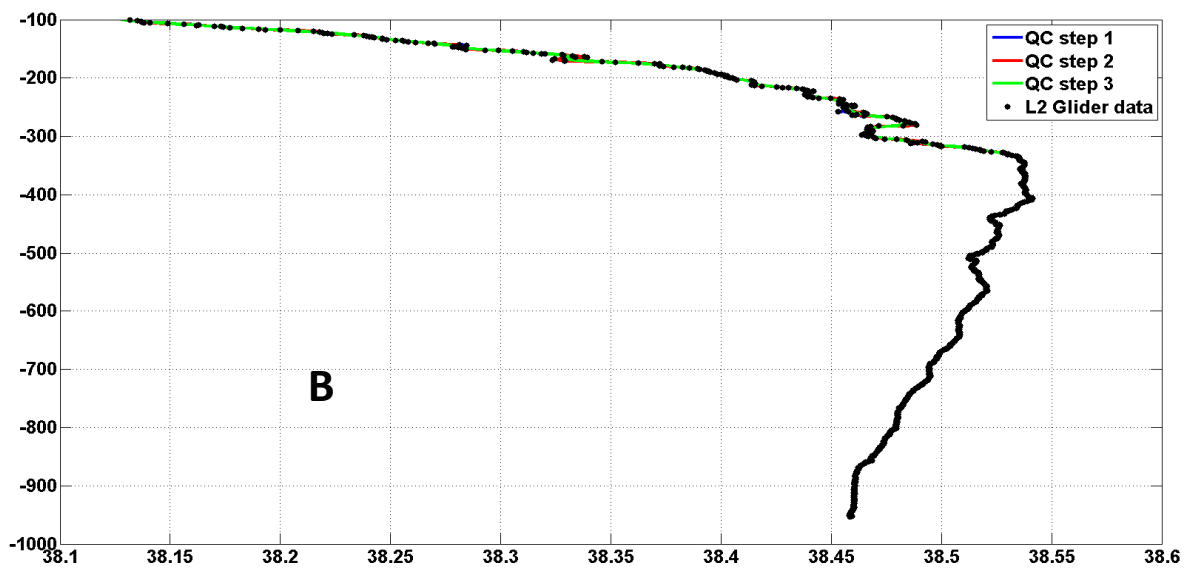
333 All dataset elaboration levels from 0 to 2 are available at <https://doi.org/10.25704/b200-3vf5>,  
334 while level 3 data are freely available upon direct request to the authors. Data samples presented  
335 in this manuscript are obtained from level 3 data.

336

337



338



339

340 *Figure 4. Effect of the additional quality control used to generate level 3 data. An example is shown*  
341 *for a salinity profile of the ABACUS 1 mission. The surface layer is shown in panel A (0-100m depth)*  
342 *while the intermediate and deep water layers are shown in panel B (from 100 to 975 m depth).*  
343 *Black dots represent the original level 2 data after the standard quality control procedures, blue*  
344 *line shows the single missing data interpolation, the median filter effect is shown through the red*  
345 *line, finally the green line represents the effect of the 5-point running mean on the data.*

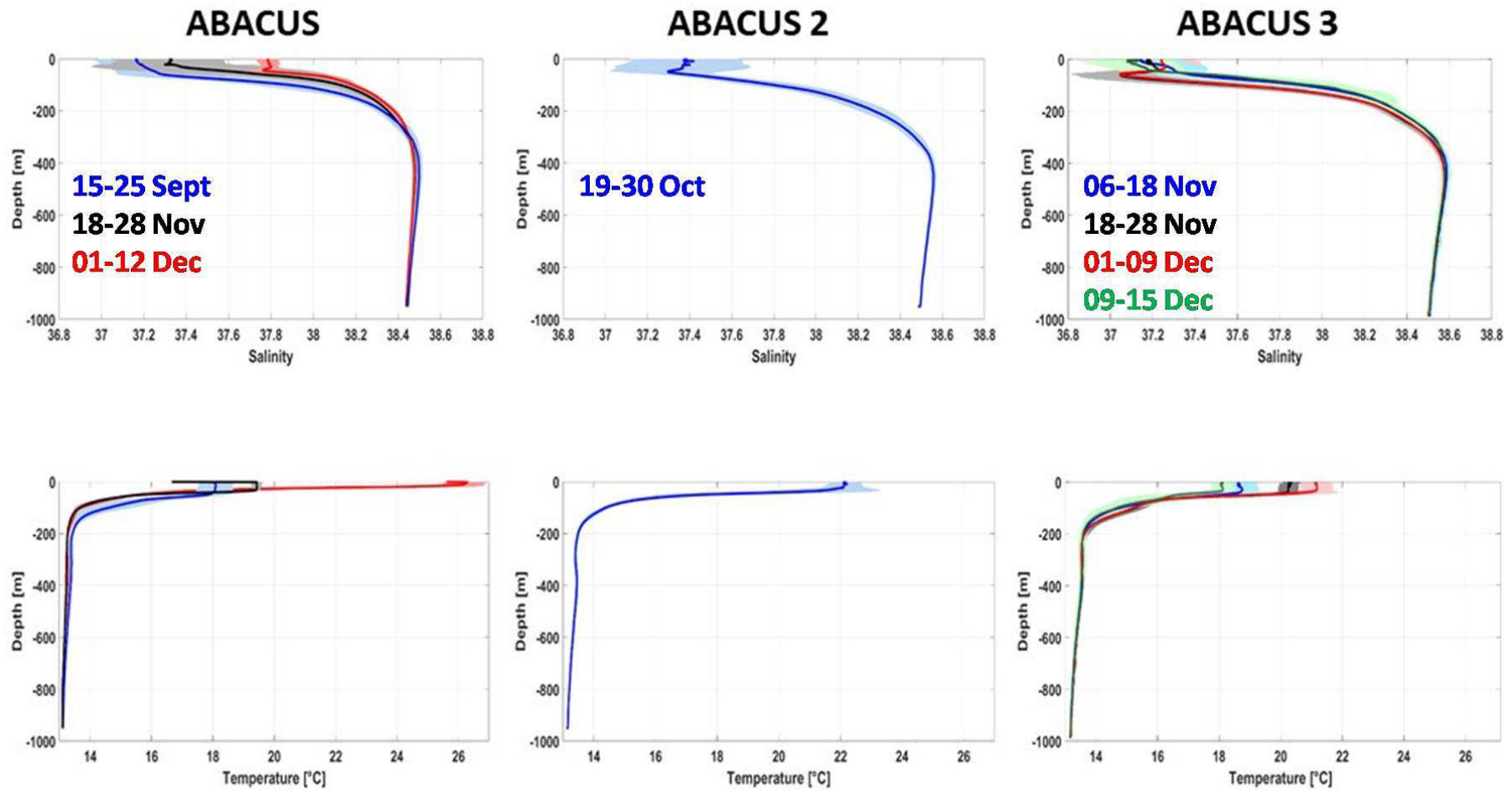
346

347

348 Figure 5 shows the mean temperature and salinity profile calculated for each transect completed  
349 during the ABACUS cruises from 2014 to 2016. For each mission, a mean profile was calculated  
350 using data of a single Mallorca-Algerian coast (or vice versa) transect. In this figure, the first  
351 available mean profile for each mission is shown in blue, the second in black, the third in red and  
352 the fourth in green. Standard deviation along depth during each transect was also computed for  
353 both temperature and salinity (shaded areas in Figure 5).

354 The ABACUS profiles are characterized by a high level of variability in the surface layer that  
355 considerably decreases in the intermediate and deeper layers, in agreement with existing  
356 literature in the area (Manca et al., 2004; Fusco et al., 2008). Salinity mean standard deviation  
357 values calculated over the entire water column for each available transect range between 0.01  
358 (ABACUS 2<sup>nd</sup> transect) and 0.04 (ABACUS 1 1<sup>st</sup> and 3<sup>rd</sup> transect; ABACUS 2; ABACUS 3 from 2<sup>nd</sup> to  
359 4<sup>th</sup> transect). Mean standard deviation values, calculated for the temperature, range between  
360 0.05°C (ABACUS 2) and 0.15°C (ABACUS 3 1<sup>st</sup>, 3<sup>rd</sup> and 4<sup>th</sup> transect). Higher standard deviation  
361 values (up to 0.43 for salinity and 7.3°C for temperature in the surface layer of ABACUS 1 1<sup>st</sup>  
362 transect and ABACUS 2 respectively) are found when single depths are considered.

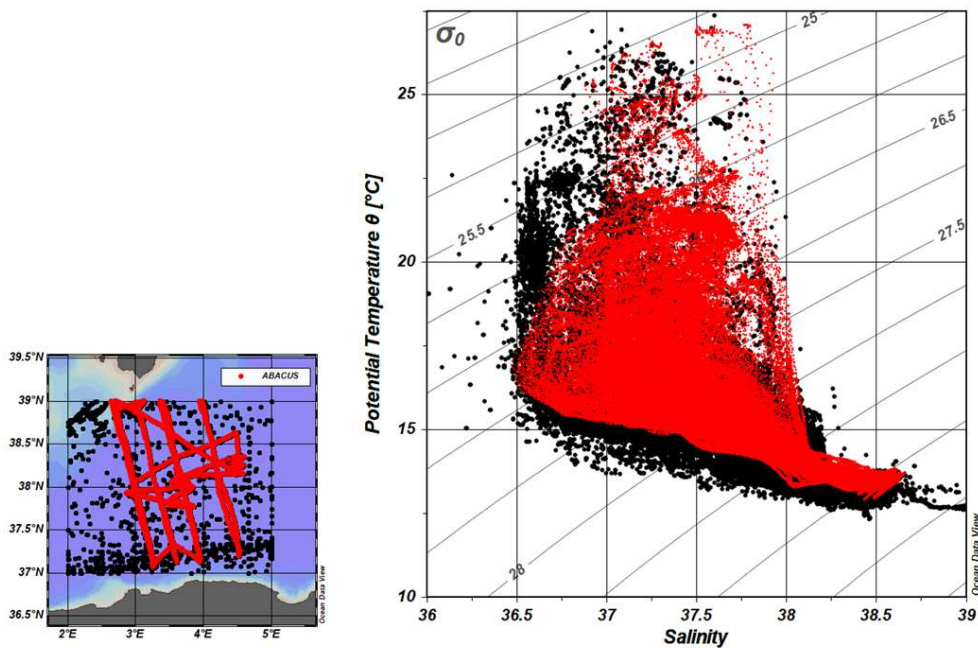
363 These values are generally larger than the precision of the glider sensors previously described  
364 (Table 1). This supports the assumption that glider measurements are accurate enough to  
365 represent the variability of the basin. Ship-based CTD profiles collected at the same time and  
366 location of the ABACUS casts and corrected to bottle samples could provide material for an  
367 interesting comparison between glider and CTD probe data, but unfortunately, no ship-based CTD  
368 data were collected in correspondence of the ABACUS missions up to 2016.



370  
 371 *Figure 5. Mean salinity (upper panels) and temperature (lower panels) profiles (thick lines) for each ABACUS transect. From left to right, ABACUS 1,*  
 372 *ABACUS 2 and ABACUS 3 data are represented. For each mission, the first available mean profile is shown in blue, the second in black, the third in*  
 373 *red and the fourth in green. Shaded area represents the standard deviation calculated at each depth for each mean profile.*

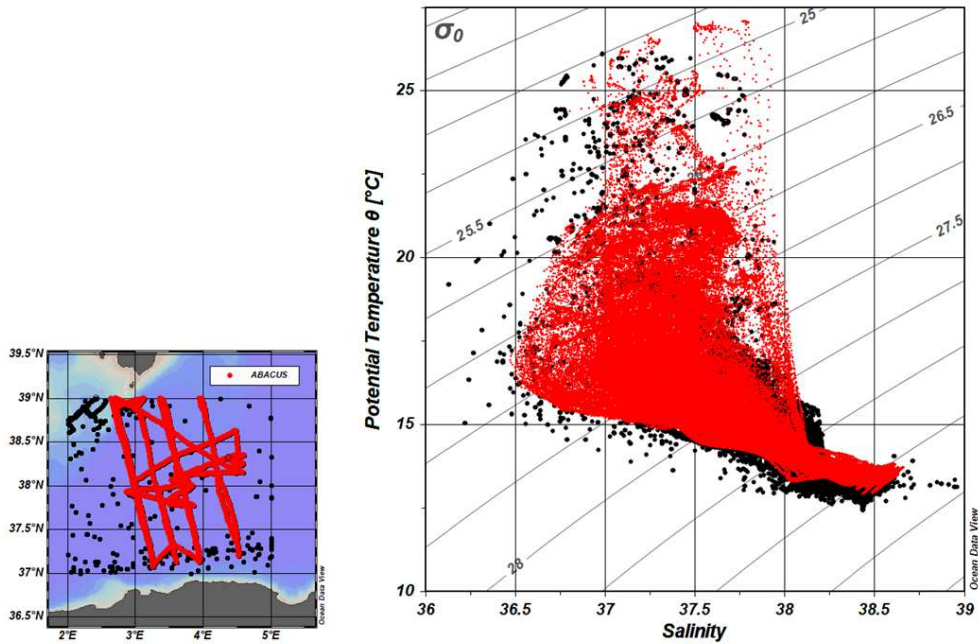
374 **4 Data comparison and transect samples**

375 In order to test the reliability of ABACUS dataset, a comparison was performed between glider  
376 data and a set of historical oceanographic measurements collected in the study area. In particular,  
377 a composite dataset including temperature and salinity data along the water column was realized  
378 merging data from the MedarMedatlas II project (MEDAR group, 2002), from the Coriolis CORA-  
379 3.4 Dataset (Cabanes et al., 2013) and from the World Ocean Hydrographic Profiles (WOHP - V1.0  
380 database, in agreement with Viktor Gouretski). The resulting dataset, consisting of about 2450  
381 profiles, spans from 1909 to 2011 with a regular distribution of the data across the different  
382 seasons. After the application of standard quality control procedures, including spike removal and  
383 the comparison among nearby profiles, the calculation of potential temperature ( $\Theta$ ) was carried  
384 out and the  $\Theta/S$  couples from this dataset and the ABACUS observations were compared.  
385 Figure 6 shows the comparison between ABACUS  $\Theta/S$  data and all the available observations in the  
386 study area. ABACUS dataset consists of 2415 profiles with the same data distribution of the  
387 historical data, and no outliers in the surface or deep layers. These results confirm that glider  
388 ABACUS data captured, and correctly describe, the main thermohaline properties of the AB water  
389 masses and their variability.  
390



391  
392 *Figure 6.  $\Theta/S$  diagram comparing historical oceanographic observations from 1909 to 2011 (black*  
393 *dots) to ABACUS data (red dots). The associated map shows the spatial distribution of the data.*  
394

395 In order to perform an additional and more accurate test on the data reliability, we selected the  
396 data collected during the fall season (September – December) from the merged historical dataset.  
397 This subset, consisting of 400 profiles was then used for a second comparison with the ABACUS  
398 data. Results are showed in the  $\Theta/S$  diagram in Figure 7. Again, the ABACUS data successfully  
399 represent the hydrographic variability of the area, even when analysing data from a selected  
400 season. Furthermore, the reduced number of historical data in the fall season and their sparse  
401 distribution are a clear indication of the relative importance of ABACUS dataset for studying the  
402 AB.  
403



404  
 405 *Figure 7.  $\theta/S$  diagram comparing historical oceanographic observations (black dots) during the fall*  
 406 *season (September – December from 1909 to 2011) to ABACUS data (red dots). The associated*  
 407 *map shows the spatial distribution of the data.*

408  
 409 Several typical Mediterranean water masses have been identified in the  $\theta$ - $S$  diagrams derived from  
 410 the glider mounted CTD during the three ABACUS missions at sea. A summary overview is  
 411 provided in Table 2. The surface layer (0 to 50 m depth) was occupied by AW whose properties  
 412 vary greatly according to different stages of mixing, precise geographical position and residence  
 413 time in the Mediterranean Sea. Potential temperature, for example, ranges between 14.4°C and  
 414 27.0°C with colder waters always identified in the southern part of the AB. More mixed and  
 415 modified waters are present in its northern sector due to the influence of Balearic waters  
 416 (Cotroneo et al., 2016). As expected, the effect of seasonal cooling can be detected too; in fact,  
 417 December missions presents lower mean surface water temperatures (below 19°C).  
 418 As for salinity, its values in the surface layer range between 36.51 and 38.04, with higher values  
 419 measured next to the Mallorca Channel, characterized by shallow bottom and easier intrusion of  
 420 saltier waters (Aulicino et al., 2018).  
 421 The intermediate layers were typically occupied by LIW, characterized by a potential temperature  
 422 generally lower than 13.5 °C, a salinity of about 38.5 and a low oxygen concentration (see an  
 423 example in Figure 8c). Its presence was mostly identified between 300 and 550 m depth.  
 424 The deepest observed layers (between 700 and 975 m depth) were usually characterized by the  
 425 presence of WMDW with typical  $\theta$  values ranging between 12.9°C and 13.2°C and salinity ranging  
 426 between 38.44 and 38.49. These waters were saltier (about 0.05) during fall 2015 and 2016 than in  
 427 the 2014 glider mission.  
 428

429  
430

Glider mission	AW	LIW	WMDW
ABACUS 1.1 15 Sept - 25 Sept 2014	$14.44 \leq \theta \leq 27.01 \text{ } ^\circ\text{C}$ $36.56 \leq S \leq 37.98$	$13.21 \leq \theta \leq 13.35 \text{ } ^\circ\text{C}$ $38.48 \leq S \leq 38.52$	$12.91 \leq \theta \leq 13.17 \text{ } ^\circ\text{C}$ $38.44 \leq S \leq 38.49$
ABACUS 1.2 18 Nov - 19 Dec 2014	$15.82 \leq \theta \leq 18.99 \text{ } ^\circ\text{C}$ $36.73 \leq S \leq 37.34$	$13.29 \leq \theta \leq 13.35 \text{ } ^\circ\text{C}$ $38.49 \leq S \leq 38.53$	$12.92 \leq \theta \leq 13.17 \text{ } ^\circ\text{C}$ $38.44 \leq S \leq 38.49$
ABACUS 2 19 Oct - 11 Dec 2015	$16.11 \leq \theta \leq 23.88 \text{ } ^\circ\text{C}$ $36.52 \leq S \leq 38.04$	$13.32 \leq \theta \leq 13.51 \text{ } ^\circ\text{C}$ $38.53 \leq S \leq 38.59$	$12.99 \leq \theta \leq 13.17 \text{ } ^\circ\text{C}$ $38.49 \leq S \leq 38.54$
ABACUS 3 4 Nov - 23 Dec 2016	$15.18 \leq \theta \leq 20.64 \text{ } ^\circ\text{C}$ $36.51 \leq S \leq 37.84$	$13.29 \leq \theta \leq 13.51 \text{ } ^\circ\text{C}$ $38.49 \leq S \leq 38.63$	$13.09 \leq \theta \leq 13.23 \text{ } ^\circ\text{C}$ $38.49 \leq S \leq 38.55$

431

432 Table 2. Temperature and salinity range values measured for Atlantic Water (AW), Levantine  
433 Intermediate Water (LIW) and West Mediterranean Deep Water (WMDW) during ABACUS 1,  
434 ABACUS 2 and ABACUS 3 missions.

435

436 The main properties of the water masses, as well as their spatial and vertical variability and  
437 distribution can be successfully observed through the analysis of vertical transects.

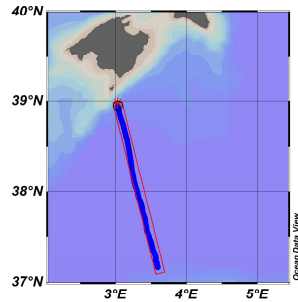
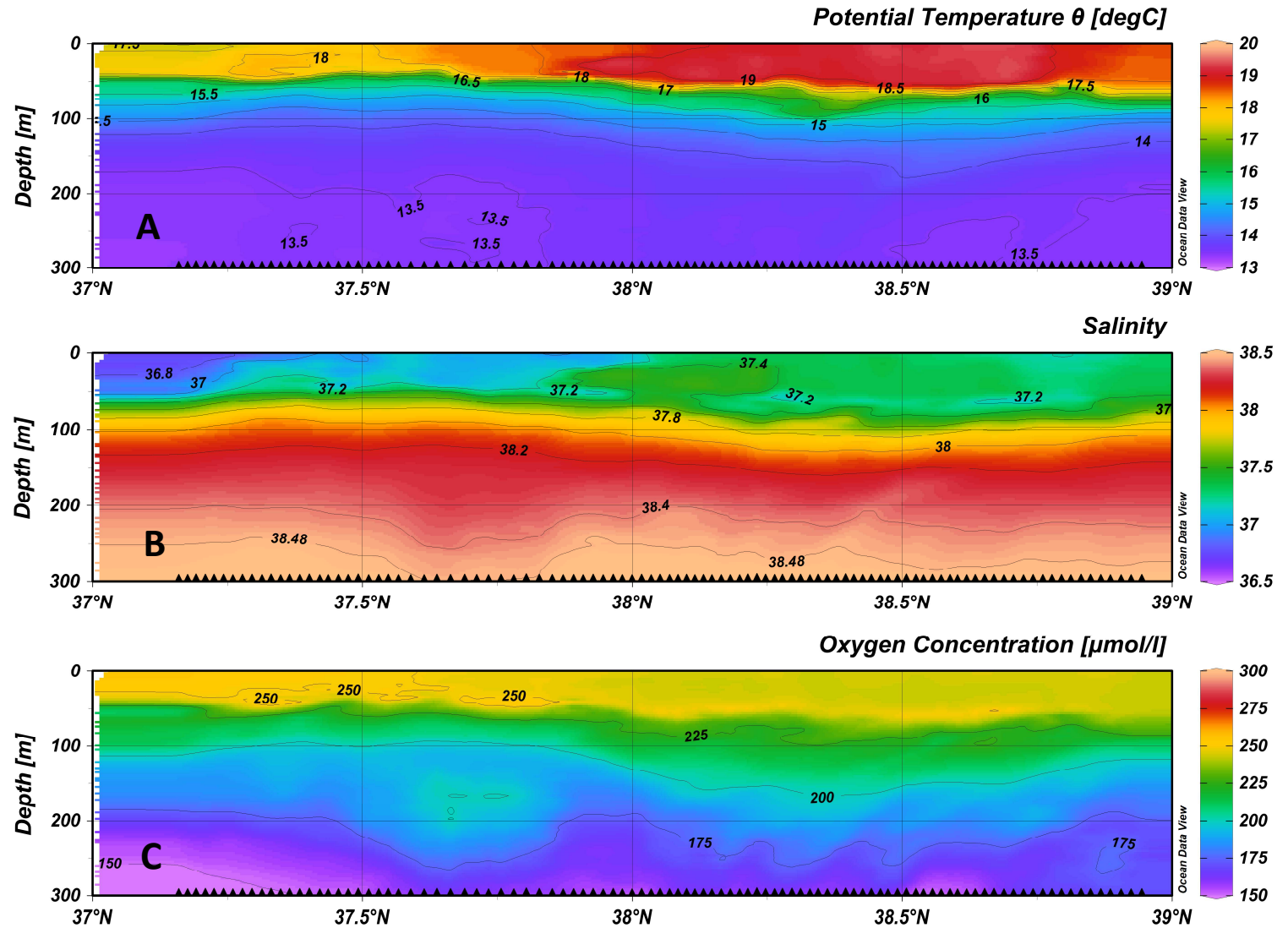
438 Figures 8 and 9 show the vertical sections along latitude of temperature, salinity, oxygen  
439 concentration, CHLA concentration and turbidity collected along the most recent transect of the  
440 ABACUS project. This North-South transect was realized during ABACUS 3, from December 1<sup>st</sup> to  
441 December 9<sup>th</sup> 2016 along the Sentinel 3 groundtrack number 713.

442 Temperature and salinity data collected in the surface layer (fig. 8 a,b) show a clear signature of  
443 the AC presence. Lower temperatures and salinities are registered in the southern part of the  
444 transect, highlighting the presence of AW recently entering the Mediterranean Sea. On the other  
445 hand, the northern part of the transect is characterized by more saline and warm waters with  
446 typical Mediterranean properties. Oxygen concentration in the surface layer presents the  
447 expected distribution, without any significant latitude pattern (Fig. 8c)

448 The North-South pattern is again evident in the CHLA concentration section (fig. 8d). An increase  
449 in the chlorophyll signal is registered in correspondence of the AC system at 50 m depth and, with  
450 lower intensity, at the northern edge of the transect where terrestrial nutrient input from the  
451 Mallorca island can be more important.

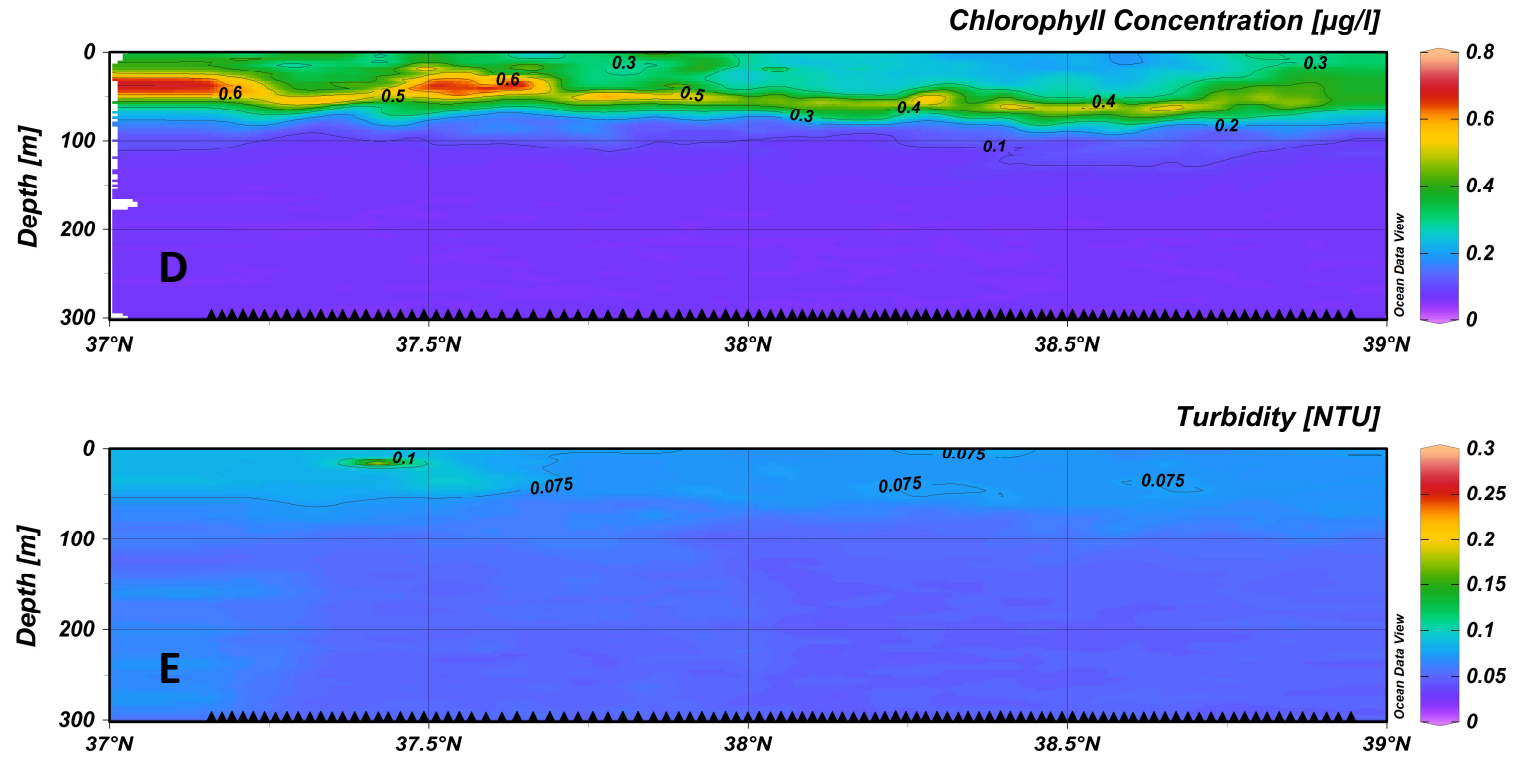
452 The CHLA concentration increase in the southern part of the transect shows the presence of a  
453 lower concentration area at about 37.3°N. This signal may be associated to meanders or filaments  
454 of the AC that deviate from the Eastward pattern of the current and impact on the biological  
455 properties of the water masses.

456 The same signal can also be identified in the temperature and salinity sections, even if with  
457 reduced intensity. The deeper layers (from 200 m to 975 m depth) are mainly characterized by the  
458 presence of the LIW. The relatively low oxygen concentration values and increased salinity signals  
459 registered between 300 and 500 m depth along most of the transect are a clear signature of the  
460 LIW presence (Fig. 9).



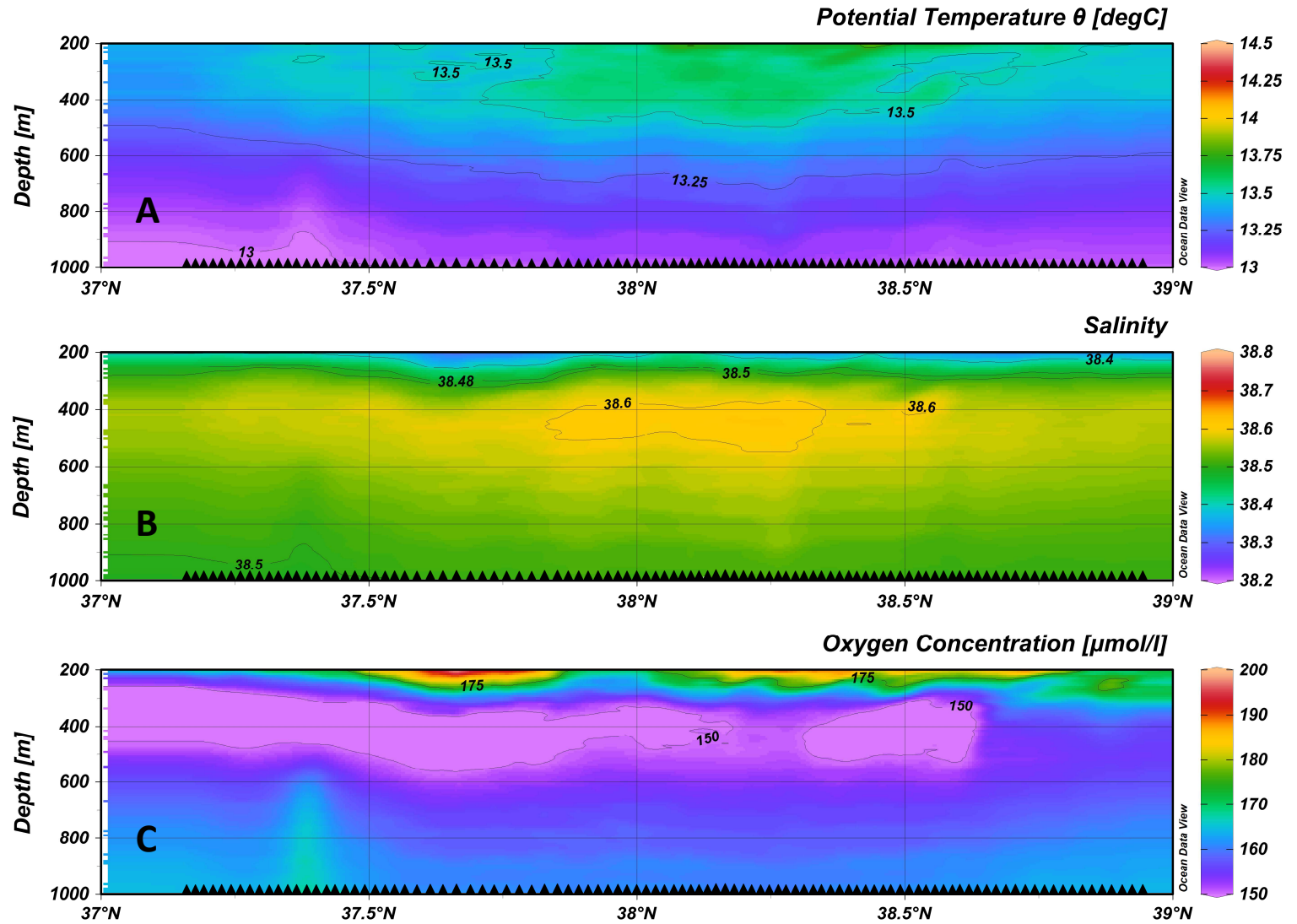
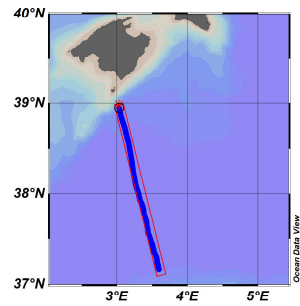
461  
 462 Figure 8. Surface layer (0-300 m depth) along track sections of potential temperature (a), salinity (b) and oxygen concentration (c) realized through  
 463 ABACUS 3 glider data. Black triangles indicate the position of the single glider profiles.  
 464  
 465





466  
467  
468

Figure 8. Surface layer (0-300 m depth) along track sections of Chlorophyll concentration (d) and turbidity (e) realized through ABACUS 3 glider data. Black triangles indicate the position of the single glider profiles.



469  
 470 Figure 9. Intermediate and deep layer (200-975 m depth) along track sections of potential temperature (a), salinity (b) and oxygen concentration  
 471 (c) realized through ABACUS 3 glider data. Black triangles indicate the position of the single glider profiles.

472 The 800-975 m depth layer, also shows the presence of a small scale structure at about 37.3°N.  
473 In this layer, a lower temperature and salinity signal associated to increased oxygen concentration  
474 can be found from 600 m to 975 m depth. This structure may be associated to the signals  
475 observed in the surface layer and surely deserves further investigations. All these data confirm the  
476 glider ability to describe the main water mass properties at all scales from basin to mesoscale and  
477 capture small scale structure along the water column and the investigated track. An example of  
478 mesoscale variability analyzed through ABACUS 1 glider data can be found in Cotroneo et al.  
479 (2016) which present the vertical sections of multiparametric observations collected across a  
480 mesoscale eddy.

481

## 482 **5 Conclusions**

483 The Mediterranean Sea is known to be particularly sensitive to changes in external forcings, thus  
484 being one of the most responsive areas to climate change (Schroeder et al., 2017; Gualdi et al.,  
485 2013) and its waters have already shown the presence of significant trends even in the deepest  
486 layers (Fusco et al., 2008; Budillon et al., 2009). In this framework, the ABACUS dataset provides  
487 about 2400 complete casts along the water column down to 975 m depth across the Algerian  
488 Basin one of the key areas of the western Mediterranean where monitoring programmes should  
489 be improved and intensified.

490 In particular, here we present data collected during a series of glider missions carried out from  
491 2014 to 2016 in the framework of the ABACUS project. This effort allowed the collection of a large  
492 dataset of physical (temperature and salinity) and biochemical (oxygen concentration, turbidity  
493 and chlorophyll concentration) high resolution in situ observations. The reliability of these  
494 measurements was tested and assessed through different quality control procedures, as well as  
495 through comparisons with available historical datasets.

496 This dataset is available through an unrestricted repository at <https://doi.org/10.25704/b200-3vf5>,  
497 where NetCDF files including different elaboration levels (from 0 to 2) and documentation are  
498 easily accessible. This multiparametric dataset is expected to be particularly beneficial to  
499 oceanographic studies focusing on the characterization of the hydrographic and biochemical  
500 structure of the Western Mediterranean at all spatial scales. In fact, the presence of AW (at  
501 different modification stages), LIW and WMDW, as well as their interannual variability, can be  
502 observed and analysed, as reported by Aulicino et al. (2018). They included part of the presented  
503 dataset in their multiplatform analyses, stressing the usefulness of glider repeated monitoring in  
504 combination with altimetry and numerical simulations. Still, these observations already proved  
505 their contribution to the analyses of the mesoscale and sub-mesoscale processes in the study  
506 region (Cotroneo et al., 2016) whose study needs to be based on an appropriate high resolution in  
507 situ dataset to possibly be coupled with satellite remote sensing data.

508 Then, we believe that the ABACUS glider dataset represents a valid unrestricted product which  
509 could partially fill the lack of information in the AB, and a valuable tool for improving, together  
510 with similar information collected in the framework of other AUV projects, our knowledge about  
511 the dynamics of the Western Mediterranean and its physical and bio-chemical characteristics at  
512 different spatial scales.

513 Moreover, we expect that this data could be used to improve and validate information derived  
514 through numerical simulations, as well as to calibrate and validate present and future satellite  
515 observations, especially those acquired through radar altimetry.

516 In a future perspective, cost efficient repeated glider cruises can then contribute to create a  
517 network of endurance lines, monitoring both the short and long-term variability of the main  
518 physical and biochemical parameters of the Mediterranean Sea. At a larger scale, the use of gliders

519 is crucial in the Global Ocean Observing System to fill gaps in transition regions between the open  
520 ocean and shelf areas (Liblik et al., 2016) and to increase the array of observations in areas  
521 traditionally lacking of in situ measurements, such as the Southern Mediterranean Sea. The  
522 synergy between multiple gliders surveys and other data sources, i.e., satellites, models, coastal  
523 radars, buoys and drifters, possibly including advisable occasional classical oceanographic cruises,  
524 could represent the best strategy to be implemented.

525 As for the AB, the ABACUS monitoring activities are expected to be repeated and enhanced during  
526 the coming years, taking into account the lesson learned through this study. From 2017 we  
527 enlarged the ABACUS network and realized more glider missions per year in order to monitor both  
528 seasonal and interannual variability along the Mallorca-Algerian coast transect.

529

### 530 **Data availability**

531 ABACUS glider data from 2014 to 2016 are available to the public in NetCDF format through an  
532 unrestricted repository at <https://doi.org/10.25704/b200-3vf5>. A set of NetCDF files for data from  
533 level 0 to level 2 is created for each glider deployment.

534 The SOCIB Data Centre hosts the data repository and offers a useful interface for data visualization  
535 and download.

536

537

### 538 **ACKNOWLEDGEMENTS**

539

540 The ABACUS 1 missions (2014) were supported by Joint European Research Infrastructure network  
541 for Coastal Observatories (JERICO) TransNational Access (TNA) third call (grant agreement No  
542 262584).

543 The research leading to ABACUS 3 (2016) was supported by the European Union's H2020  
544 Framework Programme (h2020-INFRAIA-2014-2015) (JERICO-NEXT grant agreement No. 654410).  
545 Additional EU funding (PERSEUS Grant agreement no: 287600) is acknowledged.

546 The activities described in this paper were developed in the framework of the Italian Flagship  
547 Project RITMARE

548 A.P. wishes to acknowledge support from the PRE-SWOT project (CTM2016-78607-P) funded by  
549 the Spanish National Research Program.

550 SOCIB Data Server hosts ABACUS data which are available at <https://doi.org/10.25704/b200-3vf5>.

551 The authors are particularly grateful to the SOCIB Glider Facility team and the Data Centre and  
552 Engineering and Technology Deployment staffs for their efficient cooperation.

553

554

555

556 **REFERENCES**

- 557 Alvarez, A., and Mourre, B.: Optimum sampling designs for a glider–mooring observing network, *J.*  
558 *Atmos. Ocean. Tech.*, 29, 601–612, 2016
- 559
- 560 Aulicino, G., Cotroneo, Y., Lacava, T., Sileo, G., Fusco, G., Carlon, R., Satriano, V., Pergola, N.,  
561 Tramutoli, V., and Budillon, G.: Results of the first wave glider experiment in the southern  
562 Tyrrhenian Sea. *Adv. Oceanogr. Limnol.* 7 (1), 16–35, 2016.  
563 <http://dx.doi.org/10.4081/aiol.2016.5682>.
- 564
- 565 Aulicino, G., Cotroneo, Y., Ruiz, S., Sánchez Román, A., Pascual, A., Fusco, G., Tintoré, J., and  
566 Budillon, G.: Monitoring the Algerian Basin through glider observations, satellite altimetry and  
567 numerical simulations along a SARAL/AltiKa track. *J. Mar. Sys* 179 (2018) 55–71, 2018.  
568 <https://doi.org/10.1016/j.jmarsys.2017.11.006>.
- 569
- 570 Bosse, A., Testor, P., Houpert, L., Damien, P., Prieur, L., Hayes, D., Taillandier, V., Durrieude  
571 Madron, X., D'Ortenzio, F., Coppola, L., Karstensen, J., and Mortier, L.: Scales and dynamics of  
572 submesoscale coherent vortices formed by deep convection in the northwestern Mediterranean  
573 Sea. *J. Geophys. Res.* 121, 7716–7742, 2016. <http://dx.doi.org/10.1002/2016JC012144>.
- 574
- 575 Bouffard, J., Pascual, A., Ruiz, S., Faugère, Y., and Tintoré, J.: Coastal and mesoscale dynamics  
576 characterization using altimetry and gliders: a case study in the Balearic Sea. *J. Geophys. Res.* 115,  
577 C10029, 2010.
- 578
- 579 Budillon, G., Cotroneo, Y., Fusco, G., and Rivaro, P.: Variability of the Mediterranean Deep and  
580 Bottom Waters: Some Recent Evidences in the Western Basin. *CIESM Workshop Monographs*,  
581 2009.
- 582
- 583 Carret, A., Birol, F., Estournel, C., Zakardjian, B., and Testor, P.: Synergy between in situ and  
584 altimetry data to observe and study the Northern Current variations (NW Mediterranean Sea),  
585 *Ocean Sci. Discuss.*, <https://doi.org/10.5194/os-2018-76>, 2018. In review.
- 586
- 587 Cabanes, C., Grouazel, A., Von Schuckmann, K., Hamon, M., Turpin, V., Coatanoan, C., Paris, F.,  
588 Guinehut, S., Boone, C., Ferry, N., De Boyer Montegut, C., Carval, T., Reverdin, G., Pouliquen, S.,  
589 and Le Traon, P.-Y.: The CORA dataset: validation and diagnostics of in-situ ocean temperature and  
590 salinity measurements. *Ocean Science*, 9, 1-18, 2013.
- 591
- 592 Cotroneo, Y., Aulicino, G., Ruiz, S., Pascual, A., Budillon, G., Fusco, G., and Tintoré, J.: Glider and  
593 satellite high resolution monitoring of a mesoscale eddy in the Algerian basin: Effects on the mixed  
594 layer depth and biochemistry, *J. Mar. Sys.*, Vol. 162, 73-88, 2016.
- 595
- 596 Cusi, S., Torner, M., Martinez-Ledesma, M., Roque, D., Beltran, J.P., Ruiz, S., Casas, B., Castilla, C.,  
597 Lizaran, I., Lora, S., Heslop, E., and Tintoré, J.: On the setup of an operational autonomous  
598 underwater glider facility. In: 5th MARTECH, Girona (Spain), 2013.
- 599

600 Davis, R.E., Eriksen, C.C., and Jones, C.P.: Autonomous buoyancy-driven underwater gliders. In  
601 Griffiths, G., *Technology and Applications of Autonomous Underwater Vehicles*, ed. Taylor and  
602 Francis, London, 2002.

603  
604 Drinkwater, M.R., and Rebhan, H.: Sentinel-3: Mission Requirements Document, EOPSMO/  
605 1151/MD-md, 2007.

606  
607 Escudier, R., Mourre, B., Juza, M., and Tintoré, J.: Subsurface circulation and mesoscale variability  
608 in the Algerian sub-basin from altimeter-derived eddy trajectories. *J. Geophys. Res.* 121, 6310–  
609 6322. <http://dx.doi.org/10.1002/2016JC011760>, 2016.

610  
611 Font, J., Isern-Fontanet, J., and Salas, J.: Tracking a big anticyclonic eddy in the  
612 westernMediterranean Sea, *Sci. Mar.* 68 (3), 331–342, 2004.

613  
614 Fu, L.L., and Ferrari, R.: Observing oceanic submesoscale processes from space. *EOSTrans. Am.*  
615 *Geophys. Union* 89, 489–499. <http://dx.doi.org/10.1029/2008EO480003>, 2008.

616  
617 Fusco, G., Manzella, G.M.R., Cruzado, A., Gacic, M., Gasparini, G.P., Kovacevic, V., Millot, C.,  
618 Tziavos, C., Velasquez, Z.R., Walne, A., Zervakis, V., and Zodiatis, G.: Variability of mesoscale  
619 features in the Mediterranean Sea from XBT data analysis. *Ann. Geophys.* 21, 21–32, 2003.

620  
621 Fusco, G., Artale, V., Cotroneo, Y., and Sannino, G.: Thermohaline variability of Mediterranean  
622 Water in the Gulf of Cádiz, 1948–1999. *Deep-Sea Res. I*, 55, pp. 1624–1638, 2008.

623  
624 Garau, B., Ruiz, S., Zang, G.W., Heslop, E., Kerfoot, J., Pascual, A., and Tintoré, J.: Thermal lag  
625 correction on Slocum CTD glider data, *J. Atmos. Ocean. Tech.* 28: 1065–1074, 2011.

626  
627 Gualdi, S., Somot, S., Li, L., Artale, V., Adani, M., Bellucci, A., Braun, A., Calmanti, S., Carillo, A.,  
628 Dell’Aquila, A., Déqué, M., Dubois, C., Elizalde, A., Harzallah, A., L’Hévéder, B., May, W., Oddo, P.,  
629 Ruti, P., Sanna, A., Sannino, G., Sevault, F., Scoccimarro, E., and Navarra, A.: The CIRCE simulations:  
630 A new set of regional climate change projections performed with a realistic representation of the  
631 Mediterranean Sea, *Bull. Amer. Meteor. Soc.*, 94, 65–81, doi:10.1175/BAMS-D-11-00136.1, 2013.

632  
633 Heslop, E.E., Ruiz, S., Allen, J., Lopez-Jurado, J-L., Renault, L., and Tintore, J.: Autonomous  
634 underwater gliders monitoring variability at “choke points” in our ocean system: A case study in  
635 the Western Mediterranean Sea, *Geophys. Res. Lett.*, 39, 24, 2012.

636  
637 Heslop, E. E., Sánchez-Román, A., Pascual, A., Rodríguez, D., Reeve, K. A., Faugère, Y., and Raynal,  
638 M.: Sentinel-3A views ocean variability more accurately at finer resolution. *Geophysical Research*  
639 *Letters*, 44, 12,367–12,374. <https://doi.org/10.1002/2017GL076244>, 2017.

640  
641 Isern-Fontanet, J., Olmedo, E., Turiel, A., Ballabrera-Poy, J., and García-Ladona, E.: Retrieval of  
642 eddy dynamics from SMOS sea surface salinity measurements in theAlgerian Basin (Mediterranean  
643 Sea). *Geophys. Res. Lett.* 43, 6427–6434. <http://dx.doi.org/10.1002/2016GL069595>, 2016.

644

645 Jones, C., E. Creed, S. Glenn, J. Kerfoot, J. Kohut, C. Mudgal, and Schofield, O.: Slocum gliders — A  
646 component of operational oceanography. In Proc. 14th Int. Symp. on Unmanned Untethered  
647 Submersible Technology, Lee, NH, Autonomous Undersea Systems, 2005.  
648

649 Liblik, T., J. Karstensen, P. Testor, L. Mortier, P. Alenius, S. Ruiz, S. Pouliquen, D. Hayes, E. Mauri,  
650 and K. Heywood: Potential for an underwater glider component as part of the Global Ocean  
651 Observing System. *Methods in Oceanography*, 17, 50-82, 2016.  
652

653 Manca, B., Burca M., Giorgetti A., Coatanoan C., Garcia M.-J., and Iona A.: Physical and  
654 biogeochemical averaged vertical profiles in the Mediterranean regions: an important tool to trace  
655 the climatology of water masses and to validate incoming data from operational oceanography. *J.*  
656 *Mar. Systems*, 48, pp. 83-116, 2004.  
657

658 MEDAR Group: MEDATLAS/2002 database. Mediterranean and Black Sea database of temperature  
659 salinity and bio-chemical parameters. Climatological Atlas. IFREMER Edition (4 Cdroms), 2002.  
660

661 Merckelbach, L. M., Briggs, R. D., Smeed, D. A., and Griffiths, G.: Current measurements from  
662 autonomous underwater gliders. In Proc. IEEE/OES 9th Work. Conf. Current Meas. Technol.  
663 (CMTC), Mar. 2008, pp. 61–67, 2008.

664 Merckelbach, L., D. Smeed, and Griffiths, G.: Vertical Water Velocities from Underwater Gliders. *J.*  
665 *Atmos. Oceanic Technol.*, 27, 547–563, <https://doi.org/10.1175/2009JTECHO710.1>, 2010.  
666

667 Millot, C.: Some features of the Algerian current. *J. Geophys. Res.* 90, 7169–7176, 1985.  
668

669 Millot, C.: Circulation in the Western Mediterranean Sea, *J. Mar. Sys.*, Vol. 20, pp 423–442, 1999.  
670

671 Millot, C., Candela, J., Fuda, J.L., and Tber, Y.: Large warming and salinification of the  
672 Mediterranean outflow due to changes in its composition, *Deep-Sea Res. I*, Vol. 53, pp.655–666,  
673 2006.  
674

675 Moran, X.A.G., Taupier-Letage, I., Vazquez-Dominguez, E., Ruiz, S., Arin, L., Raimbault, P., and  
676 Estarda, M.: Physical-biological coupling in the Algerian basin (SW Mediterranean): influence of  
677 mesoscale instabilities on the biomass and production of phytoplankton and bacterioplankton.  
678 *Deep-Sea Res.* 48, 405–437, 2001.  
679

680 Olita, A., Capet, A., Mahadevan, A., Claret, A., Poulain, P.-M., Ribotti, Ruiz, S., Tintoré, J., Tovar-  
681 Sánchez, A., A., and Pascual, A.: Frontal dynamics boost primary production in the summer  
682 stratified Mediterranean Sea. *Oce. Dyn.*, 67:767-782, DOI 10.1007/s10236-017-1058-z, 2017.  
683

684 Olita, A., Ribotti, A., Sorgente, R., Fazioli, L., and Perilli, A.: SLA-chlorophyll-a variability and  
685 covariability in the Algero-Provençal Basin (1997–2007) through combined use of EOF and wavelet  
686 analysis of satellite data. *Ocean Dyn.* 61, 89–102, 2011.  
687

688 Pascual, A., Bouffard, J., Ruiz, S., Buongiorno Nardelli, B., Vidal-Vijande, E., Escudier, R., Sayol, J.M.,  
689 and Orfila, A.: Recent improvements in mesoscale characterization of the western Mediterranean  
690 Sea: synergy between satellite altimetry and other observational approaches. *Sci. Mar.* 77, 19–36.  
691 <http://dx.doi.org/10.3989/scimar.03740.15A>, 2013.

692

693 Pascual, A., Ruiz, S., Olita, A., Troupin, C., Claret, M., Casas, B., Mourre, B., Poulain, P.M., Tovar-  
694 Sanchez, A., Capet, A., Mason, E., Allen, J.T., Mahadevan, A., and Tintoré, J.: A multiplatform  
695 experiment to unravel Meso- and submesoscale processes in an intense front (AlborEx). *Front.*  
696 *Mar. Sci.* 4, 39. <http://dx.doi.org/10.3389/fmars.2017.00039>, 2017.

697

698 Pessini, F., Olita, A., Cotroneo, Y., and Perilli, A.: Mesoscale Eddies in the Algerian Basin: do they  
699 differ as a function of their formation site? *Ocean Sci.* 14, 669–688, [https://doi.org/10.5194/os-](https://doi.org/10.5194/os-2017-93)  
700 2017-93, 2018.

701

702 Robinson, M., and Golnaraghi, A.: *Ocean Processes in Climate Dynamics: Global and*  
703 *Mediterranean examples. The physical and dynamical oceanography of the Mediterranean Sea,*  
704 *Kluwer Academic Publishing, 1994.*

705

706 Ruiz, S., Font, J., Emelianov, M., Isern-Fontanet, I., Millot, C., Salas, J., and Taupier-Letage, I.: Deep  
707 structure of an open sea eddy in the Algerian Basin. *J. Mar. Syst.* 33-34, 179–195, 2002.

708

709 Ruiz, S., Pascual, A., Garau, B., Pujol, M.I., and Tintoré, J.: Vertical motion in the upper ocean from  
710 glider and altimetry data. *Geophys. Res. Lett.* 36 (14), L14607, 2009.

711

712 Ruiz, S., Renault, L., Garau, B., and Tintoré, J.: Underwater glider observations and modelling of an  
713 abrupt mixing event in the upper ocean. *Geophys. Res. Lett.* 39 (1).  
714 <http://dx.doi.org/10.1029/2011GL050078>, 2012.

715

716 Rudnick, D.L.: Ocean research enabled by underwater gliders. *Annu. Rev. Mar. Sci.* 8, 519–541.  
717 <http://dx.doi.org/10.1146/annurev-marine-122414-033913>, 2016.

718

719 Rudnick, D. L., and Cole, S. T.: On sampling the ocean using underwater gliders, *J. Geophys. Res.*,  
720 116, C08010, doi:10.1029/2010JC006849, 2011.

721

722 Schroeder, K., Chiggiato, J., Josey, S.A., Borghini, M., Aracri, S., and Sparnocchia, S.: Rapid response  
723 to climate change in a marginal sea, *Sci. Rep.*, 7, 4065, [https://doi.org/10.1038/s41598-017-04455-](https://doi.org/10.1038/s41598-017-04455-5)  
724 5, 2017.

725

726 Shcherbina, A.Y., Sundermeyer, M.A., Kunze, E., D'Asaro, E., Badin, G., Birch, D., Brunner-Suzuki,  
727 A.E., Callies, J., Kuebel Cervantes, B.T., Claret, M., Concannon, B., Early, J., Ferrari, R., Goodman, L.,  
728 Harcourt, R.R., Klymak, J.M., Lee, C.M., Lelong, M., Levine, M.D., Lien, R., Mahadevan, A.,  
729 McWilliams, J.C., Molemaker, M.J., Mukherjee, S., Nash, J.D., Özgökmen, T., Pierce, S.D.,  
730 Ramachandran, S., Samelson, R.M, Sanford, T.B., Shearman, R.K., Skillingstad, E.D., Smith, K.S.,  
731 Tandon, A., Taylor, J.R., Terray, E.A., Thomas, L.N., and Ledwell, J. R.: The LatMix Summer  
732 Campaign: Submesoscale Stirring in the Upper Ocean, *Bull. Amer. Meteor. Soc.*, 96, 1257–1279,  
733 <https://doi.org/10.1175/BAMS-D-14-00015.1>, 2015.

734

735 Taupier-Letage, I., Puillat, I., Raimbault, P., and Millot, C.: Biological response to mesoscale  
736 eddies in the Algerian basin. *J. Geophys. Res.* 108 (C8), 3245–3267, 2003.

737



738 Testor, P., Send, U., Gascard, J.C., Millot, C., Taupier-Letage, I., and Beranger, K.: The mean  
739 circulation of the southwestern Mediterranean Sea: Algerian gyres. *J. Geophys. Res.* 110, C11017,  
740 2005.

741

742 Thomsen, S., Kanzow, T., Krahnemann, G., Greatbatch, R.J., Dengler, M., AND Lavik, G.: The  
743 formation of a subsurface anticyclonic eddy in the Peru-Chile undercurrent and its impact on the  
744 near-coastal salinity, oxygen, and nutrient distributions. *J. Geophys. Res. Oceans* 120.  
745 <http://dx.doi.org/10.1002/2015JC010878>, 2016.

746

747 Tintoré, J., Gomis, D., Alonso, S., and Parrilla, G.: Mesoscale dynamics and vertical motion in the  
748 Alboran Sea. *J. Phys. Oceanogr.* 21, 811–823, 1991.

749

750 Tintoré, J., Vizoso, G., Casas, B., Heslop, E., Pascual, A., Orfila, A., Ruiz, S., Martínez- Ledesma, M.,  
751 Torner, M., Cusi, S., Diedrich, A., Balaguer, P., Gómez-Pujol, L., Álvarez-Ellacuria, A., Gómara, S.,  
752 Sebastian, K., Lora, S., Beltrán, J.P., Renault, L., Juza, M., Álvarez, D., March, D., Garau, B., Castilla,  
753 C., Cañellas, T., Roque, D., Lizarán, I., Pitarch, S., Carrasco, M.A., Lana, A., Mason, E., Escudier, R.,  
754 Conti, D., Sayol, J.M., Barceló, B., Alemany, F., Reglero, P., Massuti, E., Vélez-Belchí, P., Ruiz, J.,  
755 Oguz, T., Gómez, M., Álvarez, E., Ansorena, L., and Manriquez, M.: SOCIB: the Balearic Islands  
756 coastal ocean observing and forecasting system responding to science, technology and society  
757 needs. *Mar. Technol. Soc. J.* 47, 101–117, 2013.

758

759 Troupin, C., Pascual, A., Ruiz, S., Olita, A., Casas, B., Margirier, F., Poulain, P.-M., Notarstefano, G.,  
760 Torner, M., Fernández, J. G., Rújula, M. À., Muñoz, C., Allen, J. T., Mahadevan, A., and Tintoré, J.:  
761 The AlborEX dataset: sampling of submesoscale features in the Alboran Sea, *Earth Syst. Sci. Data*  
762 *Discuss.*, <https://doi.org/10.5194/essd-2018-104>, 2018. In review.

763

764 Troupin, C., Beltran, J.P., Heslop, E., Torner, M., Garau, B., Allen, J., Ruiz, S., and Tintoré, J.: A  
765 toolbox for glider data processing and management. *Meth. Oceanogr.* 13–14.  
766 <http://dx.doi.org/10.1016/j.mio.2016.01.001>, 2016.

767

768 Vidal-Vijande, E., Pascual, A., Barnier, B., Molines, J.M., and Tintoré, J.: Analysis of a 44-year  
769 hindcast for the Mediterranean Sea: comparison with altimetry and in situ observations, *Sci. Mar.*,  
770 75(1), 71–86, 2011.

771

772 Vignudelli, S., Cipollini, P., Reseghetti, F., Fusco, G., Gasparini, G.P., and Manzella, G.M.R.:  
773 Comparison between XBT data and TOPEX/Poseidon satellite altimetry in the Ligurian-Tyrrhenian  
774 area. *Ann. Geophys.* 21, 123–135, 2003.

775

776 Webb, D.C., Simonetti, P.J., and Jones, C.P.: SLOCUM: an underwater glider propelled by  
777 environmental energy, *IEEE Journal of Oceanic Engineering*, 26, 4, 447-452, [10.1109/48.972077](https://doi.org/10.1109/48.972077),  
778 2001.